FABRICATION AND PHYSICAL CHARACTERISATION OF ZINC OXIDE THIN FILMS

by

LIM YAM TEE

Thesis submitted in fulfillment of the requirements for the degree of
Master of Science

March 2012

ACKNOWLEDGEMENTS

Since the beginning of my M. Sc candidature, many people have assisted me through the difficult times of my studies. First, I would like to thank my husband, my parents and other members of my family for their full support, encouragement and patience.

Secondly, I would like to express my deepest gratitude to my supervisor: Assoc. Prof. Dr. Saw Kim Guan for his incredible patience, support, encouragement and advice. I also like to thank my co-supervisor Prof. Dr. Kamarulazizi Ibrahim for his support.

My gratitude goes towards these people who had helped me so much during my research: The NOR Lab personnel Ms. Ee Bee Choo, Mr. Mokhtar, Mr. Hazhar, Mr. Kong, Mr. Zahari, Dr. Yam and Dr. Ng. In particular, I am thankful to the Microbiology laboratory personnel Mr. Muthu, Ms. Jamilah and Mr. Johari and all the staff of Pusat Pengajian Pendidikan Jarak Jauh.

Last but not least, I would like to thank my friends for encouraging me throughout my candidature.

TABLE OF CONTENTS

LIST OF TABLES

LIST OF FIGURES

FABRIKASI DAN PENCIRIAN FIZIKAL FILEM NIPIS ZINK OKSIDA

ABSTRAK

Filem nipis zink oksida (ZnO) telah disediakan pada permukaan subtrak sapphire α-0001 dengan menggunakan proses percikan magnetron arus terus dan disepuhlindap pada suhu berlainan dalam atmosfera lengai untuk menyiasat kesannya terhadap pancaran ultraungu (UV), tegasan, pemalar kekisi, saiz kristalit dan juga kemungkinan untuk merangsangkan pertumbuhan struktur nano. Microskop imbasan elektron (SEM) dan teknik belauan sinar-x (XRD) mendapati filem nipis ZnO mempunyai struktur butiran granular yang agak rata dengan kecenderungan orientasi paksi-c. Pengurangan intensiti puncak E_1(LO) dalam spektra Raman, peralihan dalam posisi puncak UV dan juga peningkatan dalam intensiti puncak UV selepas proses sepuhlindap menunjukkan pengurangan kecacatan dari filem-filem nipis yang dipercik. Bukti-bukti dari analisis Raman dan XRD menunjukkan pengurangan dalam nilai tegasan dan pemalar kekisi. Pengiraan saiz kristalit dengan persamaan Scherrer menunjukkan peningkatan selepas proses sepuhlindap. Dengan itu, bukti-bukti dari spektroskopi Raman dan fotoluminasi dan juga XRD mencadangkan bahawa kualiti filem nipis ZnO meningkat akibat daripada proses sepuhlindap. Rod nano dan tetrapoda diperhatikan pada filem-filem nipis yang disepuhlindap pada 800^{o}C. Perbezaan dalam saiz dan peringkat struktur nano menunjukkan bahawa pertumbuhan berlaku sepanjang proses sepuhlindap dan bukan pada permulaan sahaja. Struktur nano ZnO ini diperhatikan tumbuh dari kristalit ZnO. Satu kemungkinan yang merangsangkan pertumbuhan struktur nano ini ialah filem nipis ZnO yang dipercik adalah kaya dengan zink seperti yang ditunjukkan dalam spektroskopi Raman.

FABRICATION AND PHYSICAL CHARACTERISATION OF ZINC OXIDE THIN FILMS

ABSTRACT

Zinc oxide (ZnO) thin films were deposited on α-0001 sapphire substrates using direct current (d.c.) magnetron sputtering process and annealed at various temperatures in an inert atmosphere to investigate its effect on the ultraviolet (UV) emission, stress, lattice constants, crystallite size as well as the possibility of inducing nanostructure growth. Scanning electron microscope (SEM) and X-ray diffraction (XRD) found that ZnO thin films have a fairly uniform granular surface structure with a preferential c-axis growth direction. The reduction of the E_1(LO) peak of Raman spectrum, the shift in the UV peak position as well as the significant increase in the intensity of the UV peak after annealing indicated that the annealing process helped to reduce the defects in the sputtered ZnO thin films. Evidence from Raman and XRD analyses showed a decrease in stress and the lattice constant values. The crystallite size calculated using the Scherrer equation increased after annealing. Evidence from Raman and photoluminescence spectroscopy as well as XRD thus suggests that the quality of ZnO thin films increases as a result of annealing. Nanorods and tetrapods were observed on the thin films annealed at 800^{o}C. The different sizes and different stages of the nanostructures indicate that growth occurs throughout the annealing process and not only at its onset. The nanostructures were found to grow directly from the ZnO crystallites. A possible cause for inducing the growth of nanostructures is that the sputtered ZnO thin films are zinc-rich as indicated by Raman spectroscopy.

CHAPTER 1

INTRODUCTION

1.1 Introduction to zinc oxide (ZnO)

Zinc oxide (ZnO) thin film is a promising semiconducting material with unique properties and potential applications in optoelectronic devices. ZnO thin film exhibits good photoelectric properties with large exciton binding energy (~60meV) at room temperature and with its low cost and high reproducibility, it is widely used in variety of applications in optoelectronics such as solar cells, light emitters and laser systems. It is relatively non-toxic and thus could have important biological and medical applications. ZnO thin films is a piezoelectric material with high electromechanical coupling factor which is an important property for surface acoustic devices (Wasa and Hayakawa, 1992; Lu *et al.*, 2006). Its piezoelectric properties also makes it an attractive material for ultrasonic transducers in high-frequency region (Wasa *et al.*, 2004). Very recently, a heterojunction using a ZnO thin film on type IIb diamond was successfully fabricated (Saw *et al.*, 2010). The difficulty in making a homojunction from ZnO thin films shows that a deeper understanding on the fabrication of ZnO is needed.

Besides existing in the form of a thin film, ZnO can also exist in various types of nanostructures. ZnO thin films and nanostructures are also widely known for their applications in chemical sensing. Zhang *et al.* (2005) successfully fabricated ZnO nanorods and nanowires films with high humidity sensitivity, long term stability and fast response time. ZnO nanorods and nanowires can also be transformed into a two dimensional sensing device or as FETs in application to

adjustment of the sensing properties of sensor devices (Fryxell and Cao , 2007). ZnO nanowires that have good sensitivity to O_2 was also demonstrated (Fan *et al.*, 2004).

ZnO nanostructures are known to grow in many different physical appearances. Nanowires, nanobelts, nanorods, nanotubes, nanofibres and thin films are some of the common ZnO nanostructures. Some of the fabrication methods of ZnO thin films are molecular beam epitaxy (MBE), sputtering, chemical vapor deposition (CVD), atomic layer deposition and sol-gel method, while ZnO nanostructures such as nanorods, nanofibres and nanowires can be grown by spontaneous growth, template-based synthesis, electrospinning and lithography. Two of the most used growth processes of spontaneous growth include evaporation-condensation process and vapor-liquid-solid (VLS) growth. Evaporation-condensation process involves anisotropic growth of nanostructures and normally create single crystal nanowires and nanorods with less imperfection. The typical steps of the crystal growth process are illustrated in figure 1.1 (Cao, 2004).

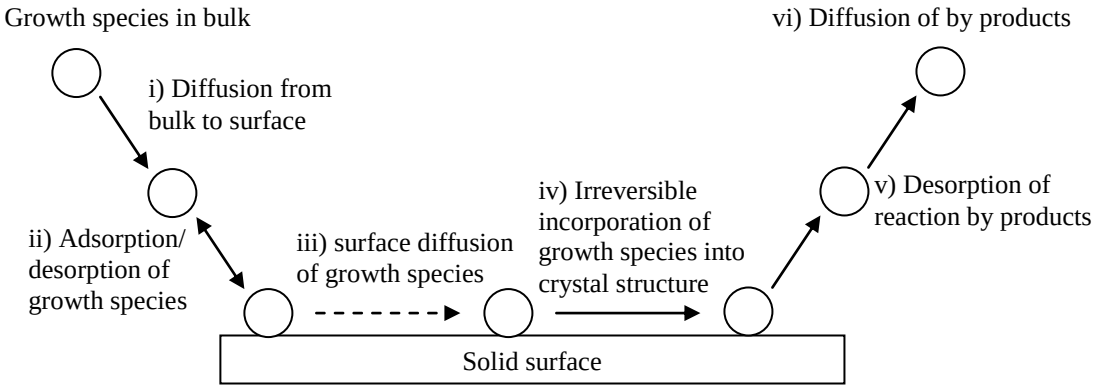

Figure 1.1. Schematic illustration of typical crystal growth process steps (adapted from Cao, 2004).

Vapor-liquid-solid (VLS) growth typically involves evaporation, diffusion, liquid droplet, precipitation, nucleation and then crystal growth. Continued crystal growth process will result in the growth of nanowires. One of the requirements of

VLS growth is the existence of a impurity or catalyst material (Wagner and Ellis, 1964). Further discussion on ZnO formation will be discussed in chapter 2.

In general, ZnO is one of the II-VI compound semiconductors with a hexagonal wurtzite structure which belongs to the space group $P6_3mc$ as shown in figure 1.2 (Wasa and Hayakawa, 1992). The ZnO wurtzite structure originated from the zinc sulfide (ZnS) or zinc blend structure. The structure consists of the zinc and oxygen atoms coordinated in an AA'BB'… method. Each atom is surrounded by four of the opposite kind atoms with a tetrahedral bonding. The zinc atom is placed at the origin 000 of the unit cell. The lattice parameters of ZnO are a = 0.3250 nm and c = 0.5207 nm (Birkholz, 2006).

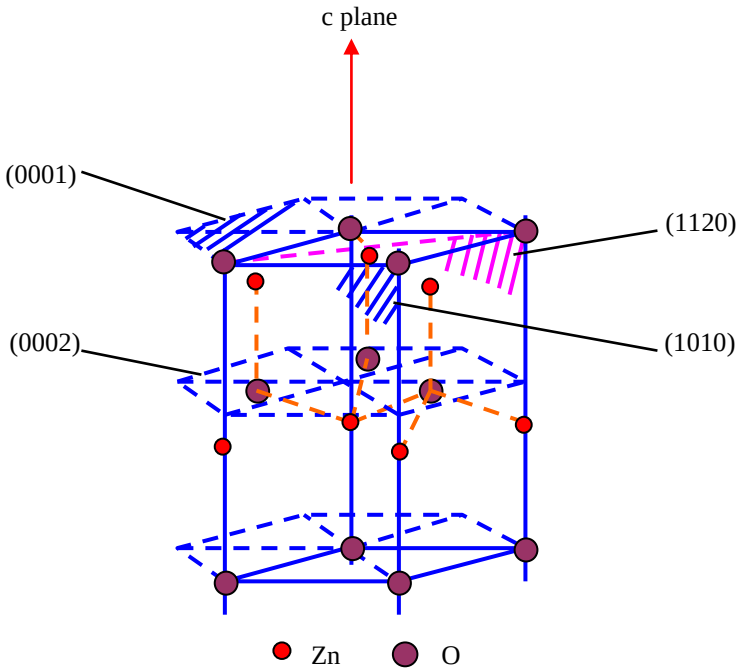

Figure 1.2. Hexagonal wurtzite structure of single crystal ZnO (adapted from Wasa and Hayakawa, 1992).

ZnO has a wide direct band gap of ~3.3 eV and shows typical n-type conductivity characteristics (Ramamoorthy *et al.*, 2004). In a direct band gap semiconductor, optical absorption process occurs directly from the valence band to the conduction band at k = 0 where k is the electron momentum as illustrated in

figure 1.3(a). For indirect band gap semiconductors, the bottom of conduction band does not lies at k = 0 as shown in figure 1.3(b) (Omar, 1975).

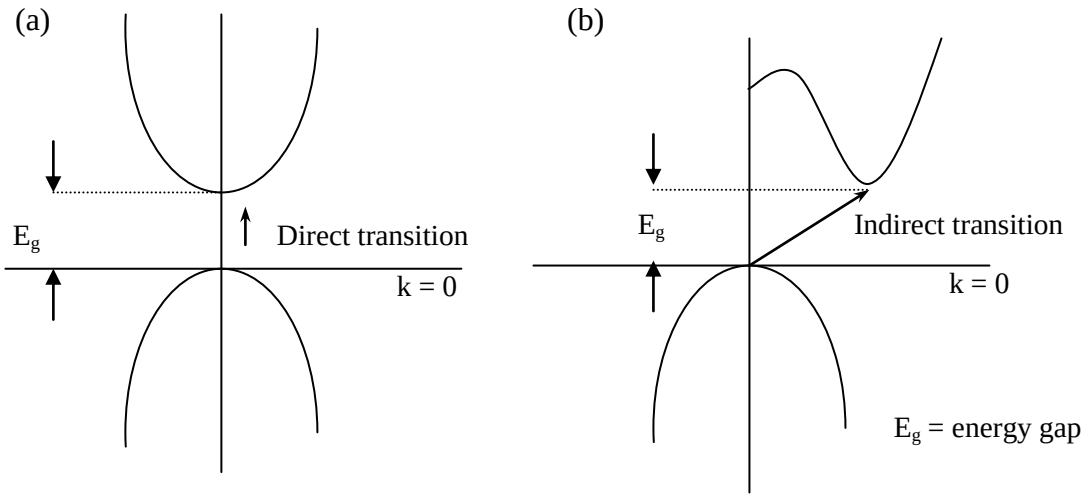

Figure 1.3. Illustration of (a) direct band gap transition, (b) indirect band gap transition (adapted from Omar, 1975).

ZnO thin films can be fabricated using several techniques on many types of substrates. The unique properties of ZnO usually depend on the fabrication techniques and the types of substrates. While it is an advantage that ZnO thin films can be fabricated using several techniques, some aspects such as associated defects and their effects on the quality of the thin films need to be investigated further. The motivation for this work comes from the ability of ZnO to exhibit various different useful properties and applications under various growth conditions. Since some growth conditions can produce nanostructures in some materials, it is also interesting to investigate the possible growth of ZnO nanostructures using a simple process such as annealing without the use of catalysts. A literature review on the unique properties of ZnO and the formation of ZnO thin films and nanostructures will be discussed in chapter 2.

1.2 Research objectives

In this work, the sputtering technique is used to deposit ZnO thin films. Deposition was performed using direct current (d.c.) magnetron sputtering instrument in an inert argon gas atmosphere. ZnO thin films will be deposited on single crystal (0001) sapphire substrate (Al_2O_3). The sputtered ZnO thin films are annealed at 700^{o}C, 800^{o}C and 900^{o}C to investigate the effect of annealing to the ZnO thin films. Since the ZnO nanostructures are known to have novel uses, we would like to investigate the possibility of growing nanostructures by using a relatively simple annealing method.

Therefore, the objectives of this research are:

1. To grow ZnO thin films using sputtering technique.
2. To characterise ZnO thin films.
3. To characterise ZnO nanostructures.

1.3 Thesis outline

In Chapter 1, the properties and potential applications of ZnO are discussed. These include the physical, electrical and optical properties that are relevant to the present study.

The general introduction to ZnO thin films and nanostructures is followed by a literature review on the findings of other researchers that are relevant to this study. Chapter 2 also includes a few of the commonly used techniques to fabricate ZnO thin films and nanostructures. The theory of ZnO thin film formation including the growth process and the conditions required are also discussed in this chapter.

Chapter 3 discusses the process of fabrication of the samples and the characterisation techniques used to investigate the samples obtained such as scanning electron microscopy, energy dispersive spectroscopy, Raman spectroscopy, photoluminescence spectroscopy and X-ray diffraction.

The results and discussions on the ZnO thin film investigation are found in Chapter 4, while Chapter 5 presents the results and discussion on the ZnO nanostructures. The results are compared to previous studies.

The last chapter, Chapter 6, gives the conclusion of the investigations on ZnO thin films and nanostructures and suggestions on future work in this area.

CHAPTER 2

LITERATURE REVIEW

2.1 Fabrication and physical characterisation of ZnO thin films and nanostructures

Due to the current interest in ZnO, intense work has been done to investigate the morphology, properties and applications of ZnO thin film. For instance, previous work by Murti and Bluhm (1982) in the orientation of ZnO films shows that it is controlled by the deposition rate. Zou *et al*. (2006) shows ZnO thin films with high crystallinity were obtained by depositing ZnO films on (100) LAO substrate using pulse laser deposition method. The transmittance of the films was high while the peaks attributed to excitons were seen in the absorption spectra (Zou *et al.*, 2006). The structure and emission characteristics were found to be influenced by the post-treatment of the deposited ZnO thin films with annealing process and bombardment process as reported by Hong *et al.* (2005). The XRD results showed both process narrowed the diffraction peak, which is a result of partial relief of residual stresses within the films. In the work by Al Asmar *et al.* (2005), ZnO films evaporated by reactive e-beam with varied film growth temperatures were found to possess the best crystallinity at 300^{o}C. The optical transmittance is the highest at 300^{o}C (Al Asmar *et al.*, 2005).

The surface morphology of ZnO films grown on Al_2O_3 was found to change significantly with growth temperature from smooth surfaces to cracks, faceted top morphology, column growth, spiral growth and micro-grains surfaces as the

temperature increases in the research by Zhang *et al.* (2004a). Figure 2.1 shows SEM images of ZnO thin film obtained by this research group.

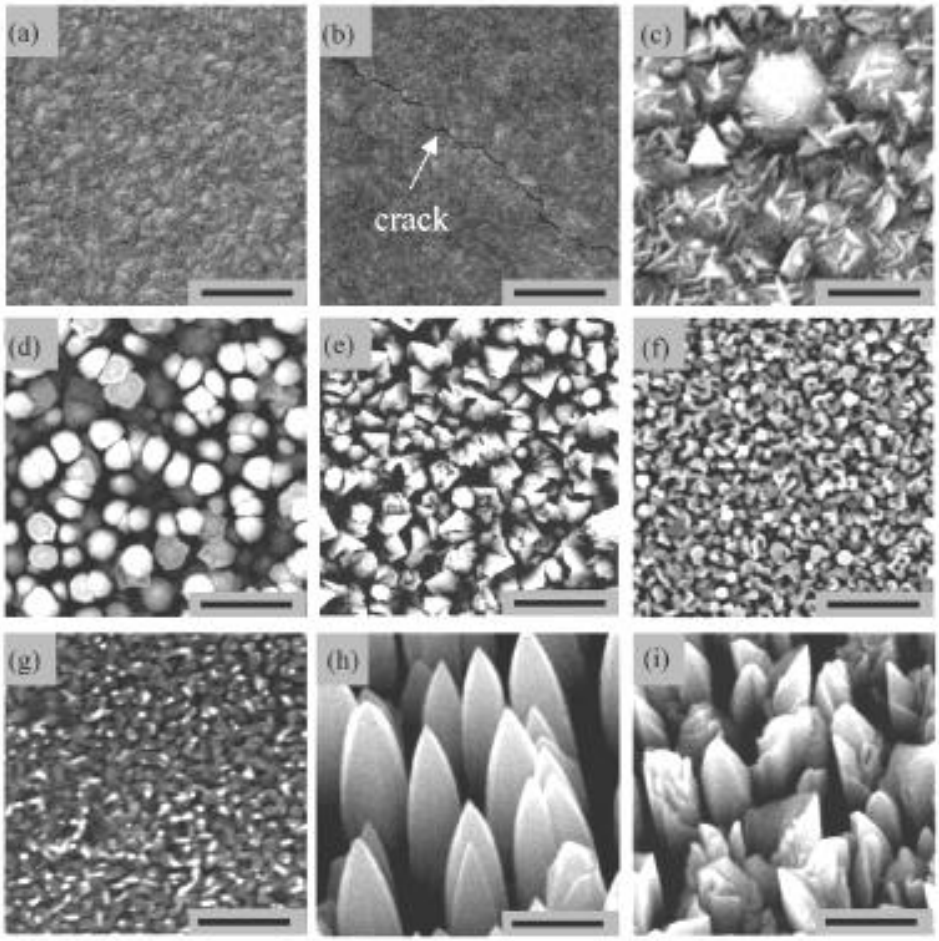

Figure 2.1. SEM images of the ZnO films on Al_2O_3. Surface SEM images of the ZnO films grown at 200 – 500°C with an interval of 50°C. (a) and (b) show smooth surfaces at growth temperature $T_g \leq 250$°C. (c), (d), (e) and (f) show facet- and column-growth at T_g=300 – 450°C. In (g), fine-grain surfaces are observed at 500°C. Cracks are observed from the film grown at T_g= 250°C. (h) and (i) show the enlarged SEM surface images of the films grown at 350 and 400°C, respectively, taken with an inclination angle of 30°. The bars indicate 1 μm in length from (a) to (f) and 0.5 μm from (g) to (i) (adapted from Zhang *et al.*, 2004a).

In the work of El-Yadouni *et al.* (2005), ZnO thin films were fabricated on sapphire substrates using metalorganic chemical vapor deposition (MOCVD). The ZnO thin films exhibit optical loss around 4 dB/cm and the guided modes indices analysis showed film thickness have good homogeneity with optical axis oriented

perpendicular to the film surface. These are the interesting properties of ZnO a potential material in integrated optics devices (El-Yadouni *et al.*, 2005).

ZnO thin films with high quality piezoelectric properties were successfully fabricated by Chen *et al.* (2004b). The ZnO thin films exhibit high resistivity over $10^6\Omega$cm and are applied in fabrication of SAW filter. In the work of Vinodkumar *et al.* (2009), ZnO thin films fabricated exhibit intense PL emission which is suitable for applications as light emitters. The ZnO thin films also exhibit high transmittance which makes it a potential window material for solar cells (Vinodkumar *et al.*, 2009).

Until present time, the fabricated ZnO thin films by deposition on most substrates have shown characteristic n-type conductivity, which is determined using Hall effect measurement. There are only a few reports of fabrication of p-type ZnO films. Zhang *et al.* (2004b) have developed p-type ZnO films by codoping nitrogen and aluminium using ultrasonic spray pyrolysis technique.

Recently, ZnO nanostructures either in shape of nanorods, nanowires or nanofibers have became an interesting field of study. In the earlier work of Li *et al.* (2005), ZnO thin films were fabricated on glass substrate by oxidation of Zn thin films that were in argon and argon/oxygen mixed gas atmosphere. The oxidation process of the Zn thin films in argon gas atmosphere showed present of nanowhiskers while the oxidation process of the Zn thin films in argon oxygen mixed gas atmosphere showed no nanowhiskers present (Li *et al.*, 2005). In the later work of Li and Gao (2007), growth of ZnO nanostructures was prepared by wet oxidation. A Zn-based precursor film was first prepared by magnetron sputtering. Then the Zn-based precursor film undergo wet oxidation at a temperature of 300 – 600^oC with water content of 5% – 70% with O_2 atmosphere. Nanostructures in the

form of nanowhiskers, nanorods, nanowires and nanobelts were observed (Li and Gao 2007).

In a research by Riley *et al.* (2007), nanostructures were formed by depositing a ZnO thin film through pulse laser deposition using an aqueous solution of $Zn(NO_3)_2$ and hexamethylenetetramine (HMT) at temperature 90 ℃ for a period of 10 hours. Figure 2.2 shows the images of nanostructures obtained by Riley *et al.* (2007). This work by Riley *et al.* (2007) is important as it shows that nanostructures can be fabricated from ZnO thin films. An interesting question would be whether ZnO nanostructures can be grown from ZnO thin films without the use of aqueous solutions.

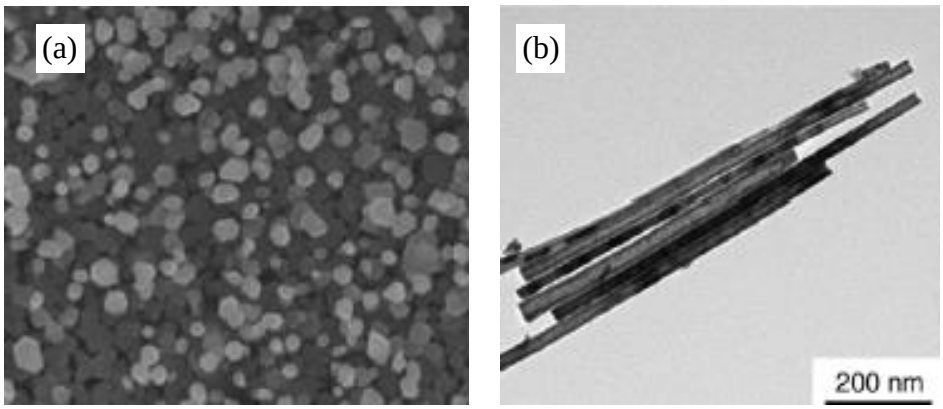

Figure 2.2. Electron microscope images of ZnO nanoarrays. Samples were removed from the reaction solution at different times. (a) A plan view SEM image of a substrate removed from the reaction solution after 2hrs. (b) A TEM image of the nanotubes formed on the substrate after 10hrs immersion (adapted from Riley *et al.*, 2007).

In another research by Huang *et al.* (2001), ZnO nanowires were synthesized using vapor phase transport and condensation process. These researchers are able to pattern the nanowire growth by using Au as the catalyst with the potential of fabricating nanoscale light emitters (Huang *et al.*, 2001). Nanomaterials also exhibit

high-humidity sensitivity, good long-term stability and fast response time (Zhang *et al.*, 2005).

ZnO crystal fibers were grown by using ZnO and carbon powders as reactants through thermal vapor method in air at temperature of 1100^{o}C by Chen *et al.* (2004a). Figure 2.3 shows SEM images of the crystal fibers obtained by the research group. The crystal fibers were found to be hexagaonal wurtzite phase ZnO with good crystallinity through the XRD and Raman spectra. The growth was explained using the thermal chemical reaction and VLS growth mechanism

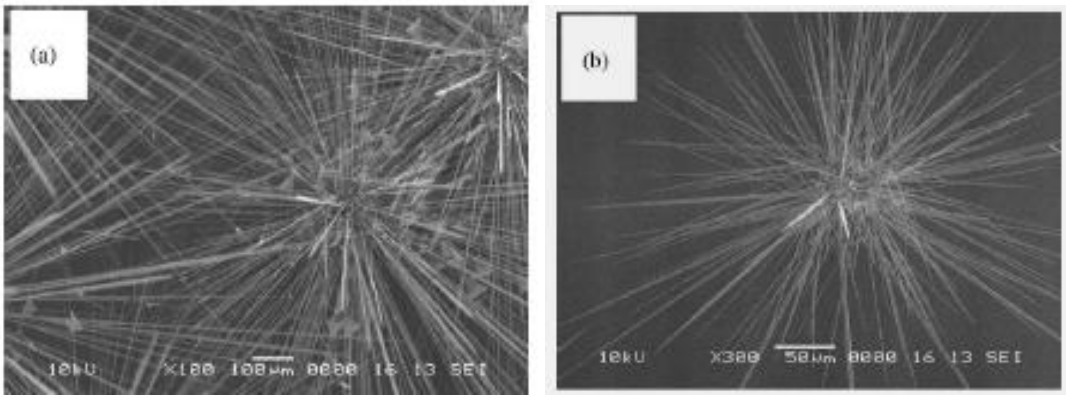

Figure 2.3. SEM images of the ZnO crystal fibers on silicon substrate. (a) Magnification of x100. (b) Magnification of x300 (adapted from Chen *et al.*, 2004a).

Interestingly, ZnO nanowires were able to grow from direct heating of brass in air (Xiao *et al.*, 2008). The nanowires obtained from this direct heating process also exhibit longer stability in field emission. It was proposed that the contact between brass substrate and ZnO nanowires is a low-resistance Ohmic contact (Xiao *et al.*, 2008).

Xu *et. al.* (2008) successfully synthesized uniform ZnO nanorods that exhibit excellent response and stability to ethanol compared to ZnO nanoparticles using gas

sensing measurement. These properties make the nanostructures promising material for producing gas sensor of better stability and sensitivity (Xu *et al.*, 2008).

In the work of Li *et al.* (2010), ZnO nanorods on ZnO nanofibers homogeneous hierarchical nanostructures were fabricated using a combined process of electrospinning and hydrothermal reaction. They found that as the density of ZnO nanorods on the surface of ZnO nanofibers increased, so does the responsivity of the UV and visible. These properties makes the nanostructures a potential material in the application of UV and visible light detector (Li *et al.*, 2010). Another interesting ZnO nanostructure formation is the tetrapods. Wang *et al.* (2005a) had successfully synthesised tetrapod-like ZnO nanostructures by thermal evaporation process on zinc powder with substrate Si.

Although a major part of this present work is on the fabrication and physical characterisation of ZnO thin films, it would be interesting to look into the possibility of various types of ZnO nanostructures that could grow on the ZnO thin films.

2.2 Formation of ZnO thin films

In this work, the growth of ZnO thin film on sapphire substrates involves heterogeneous nucleation. Heterogeneous nucleation is a process where a new phase of a particular material is formed on the surface of another material. In heterogeneous nucleation, the vapor growth species will impinge on the growth surface or substrate and form a cluster through diffusion and aggregation. These will cause a change in the chemical energy, ΔG due to the decrease in the Gibbs free energy and increase the surface or interface energy. ΔG is given by (Cao, 2004):

$$\Delta G = a_3 r^3 \Delta\mu_v + a_1 r^2 \gamma_{vf} + a_2 r^2 \gamma_{fs} - a_2 r^2 \gamma_{sv} \qquad (2.1)$$

where r = mean dimension of cluster

$\Delta\mu_v$ = change of Gibbs free energy per unit volume

γ_{vf}, γ_{fs}, γ_{sv} = surface or interface energy of vapor-cluster, cluster-substrate and substrate-vapor interface

a_1, a_2, a_3 = geometric constants

In order to obtain a stable cluster, the size of cluster must be larger that critical size r* which is given by:

$$r^* = \frac{2\pi\gamma_{vf}}{\Delta G_v}\left\{\frac{\sin^2\theta\cos\theta + 2\cos\theta - 2}{2 - 3\cos\theta + \cos^3\theta}\right\} \qquad (2.2)$$

Where θ is the contact angle that is define by Young's equation : $\gamma_{sv} = \gamma_{fs},+ \gamma_{vf}\cos\theta$

From the critical size, a critical energy barrier ΔG^* can be obtain:

$$\Delta G^* = \left\{\frac{16\pi\gamma_{vf}}{3(\Delta G_v)^2}\right\}\left\{\frac{2 - 3\cos\theta + \cos^3\theta}{4}\right\} \qquad (2.3)$$

For synthesis of nanoparticles on a substrate, θ must be > 0, and the Young's equation becomes: $\gamma_{sv} < \gamma_{fs},+ \gamma_{vf}\cos\theta$.

Growth of thin films was derived into 3 basic modes: 1. Island growth (Volmer-Weber growth), 2. Layer growth (Frank-van der Merwe growth), and 3. Island-layer growth (Stranski-Krastonov growth). Island growth involves growth species which preferred to bound with each other than to the substrate. A good example of the Volmer-Weber growth mode is given by Saw *et al.* (2003) which shows that the bond between the growth species of diamond are stronger than the bond between the growth species and the underlying sapphire substrate. This subsequently caused the diamond thin film to delaminate from the sapphire growth. Layer growth involves growth species which preferred to bound with substrate than each other. Island-layer growth is in the intermediate conditions between island growth and layer growth. Island-layer growth will develop stress within the thin film

fabricated due to the lattice mismatch (Chambers, 2000). A modified island-layer growth mode has been used to explain the growth of heteroepitaxial ZnO nanostructures (Shi and Wang, 2010)

There are other conditions that will affect the overall volume of Gibbs free energy such as deposition with cleavage steps and screw dislocation that can cause stress release and reduced the energy barrier, and the change of surface, electrostatic and chemical energy due to the existence of surface charge and impurities (Cao, 2004).

Apart from volume of Gibbs free energy, the deposition temperature and the impinging rate of deposit will also affect the formation of the film. The film developed can be a single crystal film, amorphous film or polycrystalline film. To develop a single crystal film, it needs a clean single crystal substrate, high growth temperature to ensure sufficient mobility of growth species and low impinging rate to ensure sufficient impinging time. For amorphous film, it needs a low growth temperature and high influx of growth species onto the growth surface so that there is no time for the growth species to look for the growth site with the lowest energy. As for polycrystalline films, its development conditions are in between single crystal film and amorphous film where moderate temperature and moderate high impinging flux is required (Cao, 2004).

In this work, ZnO oxide thin films were deposited using sputtering technique which is one of the most favorable techniques used by researchers due to its easy handling, low cost development and stability throughout the deposition process. Sputtering involves the process of energetic ions knocking out the atom or molecule of the target (cathode electrode) and depositing on the substrate (anode electrode). In a typical direct current (d.c.) sputtering, the target and substrate are placed facing

each other in the sputtering chamber as shown schematically in figure 2.4 (Wagendristel and Wang, 1994).

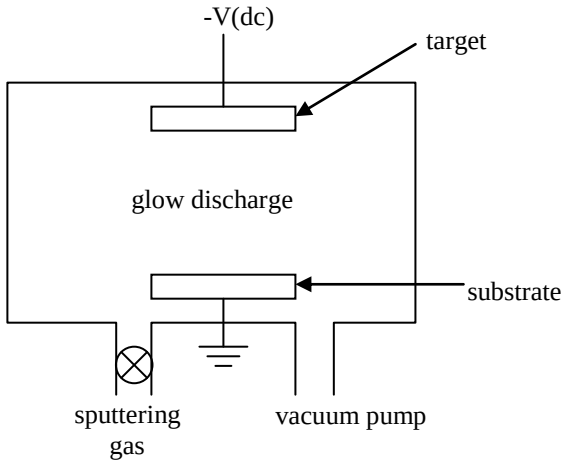

Figure 2.4. Schematic diagram of a typical d.c. sputtering system (adapted from Wagendristel and Wang, 1994).

When a d.c. voltage is introduced to the electrodes, it creates a glow discharge between the electrodes. The free electrons will accelerate because of the electric field and will obtain enough energy to ionise the sputtering gas. The sputtering gas used is normally an inert gas such as Argon. The positively charged Ar ions will strike the cathode, which is the target to eject neutral target atoms through momentum transfer. These atoms will deposit themselves on the substrate which is mounted on the anode. Other than the growth species, other negatively charged species will also interact with the substrate or grown film due to the effect of the electric field. There are modifications that have been made to the sputtering system to improve the deposition process. A magnetic field is applied to the sputtering system so that the growth species stay in vapor phase longer to able to search for the most suitable deposition site which is the lowest energy site. This modification is known as magnetron sputtering,

Surface morphology of the ZnO thin films can be investigated using SEM while other physical properties can be studied by other techniques such as X-ray diffraction, Raman spectroscopy and photoluminescence spectroscopy.

2.3 Formation of ZnO nanostructures

The formation of ZnO nanostructures can be induced by spontaneous growth, template-based synthesis, electrospinning and lithography. Here we will concentrate on spontaneous growth, which is the most probable cause of the results obtained for this work since no catalysts are intentionally added in the growth process. The commonly found spontaneous growth include evaporation-condensation growth, vapor-liquid-solid (VLS) growth and stress-induced recrystallisation.

Evaporation-condensation growth produces nanowires and nanorods through anisotropic growth. Anisotropic growth can be caused by the different growth rate of different facet of the crystal, existence of imperfection such as screw dislocation in a specific crystal direction , preferential accumulation of impurities on specific facets and also the difference accommodation coefficients in different facets. In a crystal material, different facets have different atomic density and atoms on different facets have different number of broken bonds which leads to different surface energy. This will create different growth mechanisms and growth rates. The Periodic Bond Chain (PBC) theory categorized the facets into 3 groups: flat surface, stepped surface and kinked surface (Hartman and Perdok, 1955a, 1955b, 1955c).

For flat surface, the step growth theory (also known as KSV theory) stated that when an atom adsorbs onto a surface, diffusion occurs. If the diffusion is on energetically favorable site, the atom incorporated into the crystal structure causing the surface growth. It is very likely that there are different sites with different energy

levels on the growth surface of the underlying substrate. The atoms incorporated on different sites create different chemical bonds. For example, an atom adsorbs on a terrace site might have only one chemical bond and the atom might escape back to vapor phase. Other sites such as ledge sites, ledge-kink sites and kink sites create more chemical bonds with the adsorb atom and the incorporations are irreversible. These sites are the growth sites which will cause the growth on the surface. The limitation of this theory is when the growth sites are fully consumed or used up there will be no more growth site for further growth of nanostructures. However, the presence of screw dislocations can act as a continuous source to generate growth sites so that the stepped growth or kink growth can continue. The fact that different facets have different ability to accommodate dislocations result in anisotropic growth that leads to the nanowires and nanorods formation (Heying *et al.*, 1999).

The vapor-liquid-solid (VLS) growth was first proposed by Wagner and Ellis (1964). In the VLS growth, a catalyst or impurities in the form of liquid or solution is introduced to direct and confine the crystal growth. The process of VLS growth started with the evaporation of the growth species, followed by diffusion and dissolves into liquid droplet that has a large accommodation coefficient which is the preferred site for surface growth. The growth species in the liquid droplet will saturate and undergo diffusion and nucleation at the interface between substrate and liquid to result in crystal growth. The continual growth will separate the substrate and the liquid droplets induce the formation of nanowires. The size of the nanowires can be controlled by the size of the liquid catalyst droplets which can be controlled by the thickness of the catalyst films on the substrate. This means that the thinner film forms smaller droplets which in turn create a smaller diameter nanowires although there is a minimum size limit of the liquid droplets (Wagner and Ellis, 1964,

1965). An example of the VLS growth was reported by Zhu *et al.* (2005), where the ZnO nanowires were grown through VLS using Au and Ag as catalysts. Another type of process of growing nanostructures involves stress-induced recrystallisation. This process applies pressure on solids at elevated temperatures. The growth rate appears to be proportional to the pressure applied. The site of growth is at a dislocation at the base of the nanostructure (Eshelby, 1953; Frank, 1958).

In the following chapter, the details of the fabrication process and characterisation techniques are discussed.

CHAPTER 3

METHODOLOGY OF THE FABRICATION AND CHARACTERISATION TECHNIQUES

3.1 Fabrication techniques

ZnO films can be deposited using a variety of techniques such as spray pyrolisis (Krunks and Mellikov, 1995), pulsed laser deposition (Zou *et al.*, 2006), chemical vapor deposition (Wang *et al.*, 2005b; Zhang *et al.*, 2004a) and sputtering technique (Chen *et al.*, 2004b; Lin *et al.*, 2005). One of the commonly used techniques is sputtering due to its high possibility of obtaining good orientation and uniform films (Fang *et al.*, 2005). Chen *et al.* (2004b) has fabricated a highly c-axis oriented ZnO thin film on Si substrate using dc reactive magnetron sputtering in Ar/O_2 mixture gas atmosphere. In this study, ZnO thin films were fabricated using sputtering technique and annealed at various temperatures.

3.1.1 Sputtering theory

Sputtering is a phenomenon of a solid surface is bombarded with energetic particles such as accelerated ions (Wasa and Hayakawa, 1992). In magnetron sputtering, a magnetic field is superposed on the cathode and glow discharge, which is parallel to the cathode surface. The electrons in the glow discharge shows cycloidal motion and the center of the orbit drifts in a direction of **E** x **B** with the drift velocity of **E**/**B**, where **E** and **B** denote the electric field in the discharge and the superposed transverse magnetic field respectively. The magnetic field is oriented such that these drift paths for electrons form a closed loop. This electron trapping

effect increased the collision rate between the electrons and the sputtering gas molecules. This enables one to lower the sputtering gas pressure as low as 10^{-4} Torr, but more typically 10 mTorr (Wasa and Hayakawa, 1992).

Sputtering yield (Sy) is defined as the mean number of atoms removed from the surface of the target per incident particle:

$$Sy = \frac{\text{atoms removed}}{\text{incident particle}} \qquad (3.1)$$

The sputtering yield is influenced by the structure and composition of the target material, the parameters of the incident particle and experimental geometry.

The d.c. magnetron sputtering needs a lower voltage operation than simple dc sputtering and a lower operating pressure (Ohring, 2002). It can also avoid gas phase collisions and scattering at high pressure, which randomize the directional character of the sputtered atom flux and lower the deposition rate. A fundamental reason for these beneficial effects in magnetron is the displacement of the Paschen curve to lower Pd values relative to simple discharges. Therefore, for the same electrode spacing and minimum target voltage, a stable discharge can be maintained at lower pressures (Ohring, 2002). The most commonly used dc magnetron sputtering machine is the planar post magnetron sputtering machine and the cylindrical-post magnetron sputtering machine.

Finally, in the magnetron sputtering system, the magnetic field increases the plasma density, which leads to increase of the current density at the cathode target, effectively increasing the sputtering rate at the target. Due to low working pressure, the sputtered particles traverse the discharge space without collisions, which results in effectively a higher deposition rate than higher pressure deposition systems (Wasa and Hayakawa, 1992).

3.1.2 Sputtering process

The d.c. magnetron sputtering instrument used in this research is the cylindrical-post magnetron sputtering. The sputtering system used was Edward Auto 306 DC Sputtering system (Figure 3.1).

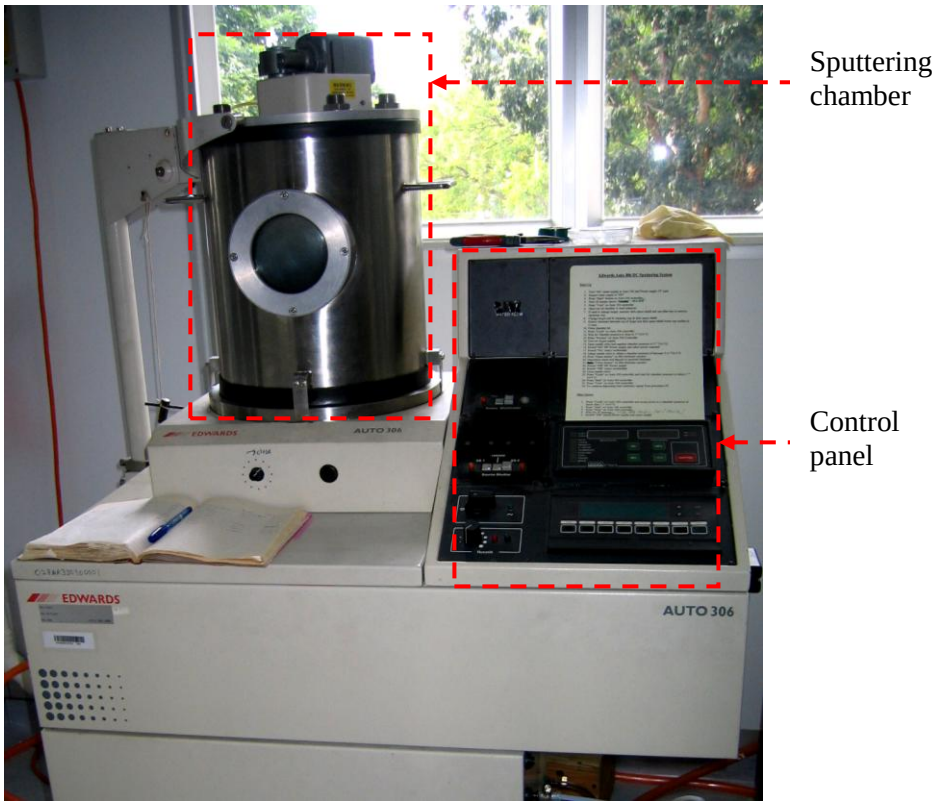

Figure 3.1. The Edward Auto 306 DC Sputtering Instrument.

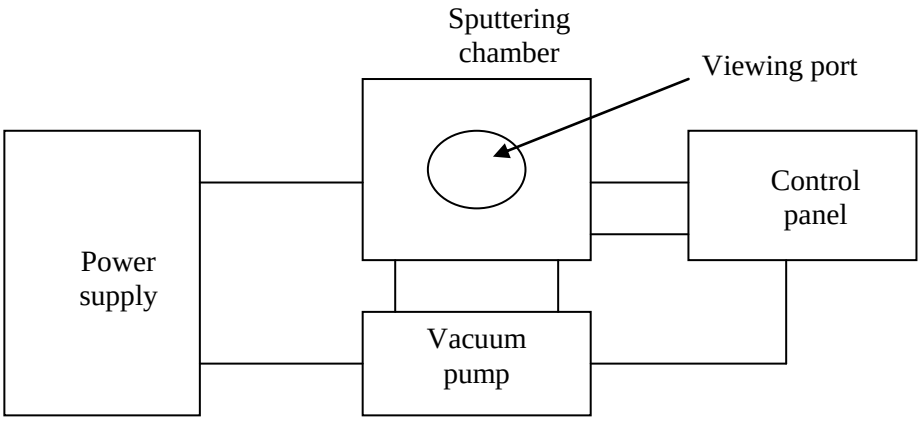

Figure 3.2. Schematic diagram of the Edward Auto 306 DC sputtering system.

The sputtering instrument generally consists of 4 sections: the power supply, vacuum pump system, controlling system and the sputtering chamber as illustrated in figure 3.2. The power supply will provide the power needed for the sputtering process. The vacuum pump system is an oil vapor rotary vacuum pump. It has the capability of pumping the chamber pressure to as low as 5×10^{-5} Torr. The controlling system will control the operation of the sputtering process. It also shows the deposition rate of the sputtering process. The sputtering chamber consists of rotary work holder and a base plate where the magnetron cathode and the shutter are mounted. There is also a viewing port in front of the sputtering chamber for the sputtering process to be seen from outside the chamber.

The substrates used in this experiment are single crystal 0001 sapphire (α-Al_2O_3). Sapphire is commonly used for deposition due to its chemical inertness, hardness properties, transparent nature and good thermal endurance (Saw, 2004). Ultrasonic cleaning technique is used to clean the substrates. The substrates are first cleaned with distilled water, rinsed with ethanol and then with acetone in a clean beaker. Then, the substrates are placed into another clean beaker containing acetone and the beaker is place into the ultrasonic cleaner and cleaned for 30 minutes. After that, the substrates are taken out and dried with pure nitrogen blower.

Figure 3.3 is the schematic diagram of the deposition chamber. Before starting the deposition, the work holder plate must be cleaned to remove any unwanted materials from previous experiments. This is to avoid possible contamination on the thin films to be produced. After the work holder is cleaned, the sputtering chamber is gently wiped with a piece of “Kim Wipes” dust free paper. The substrates are then mounted onto the rotary work holder plate of the sputtering

machine. Power of sputtering was set to 220W. A circular shape sintered zinc oxide target of 99.99% purity with diameter of 3 inches as shown in figure 3.4 was used.

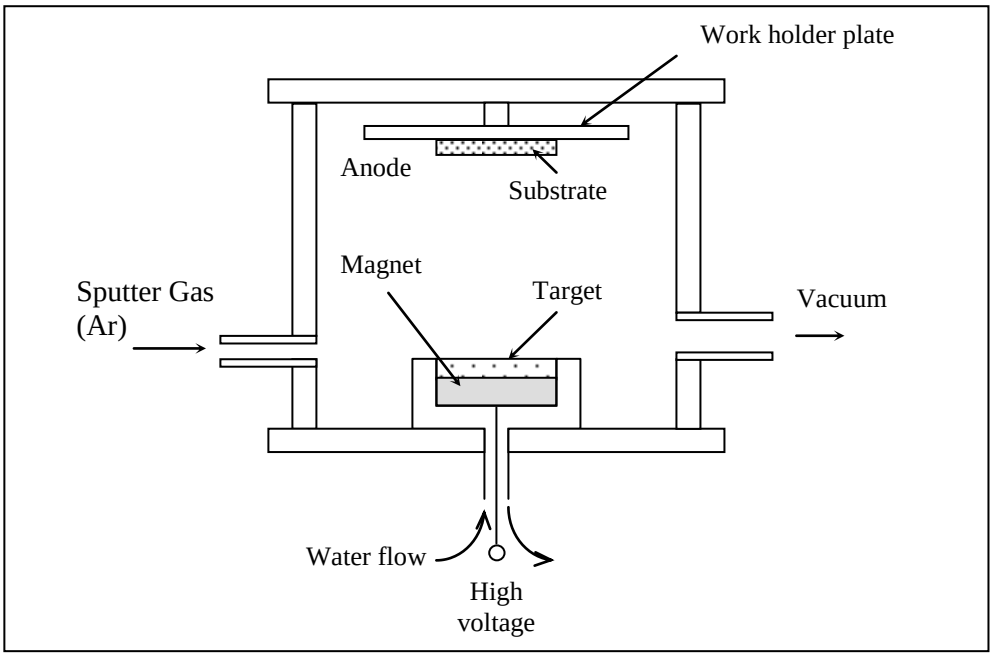

Figure 3.3. Schematic diagram of the sputtering chamber. The flow of water is to keep the target from overheating.

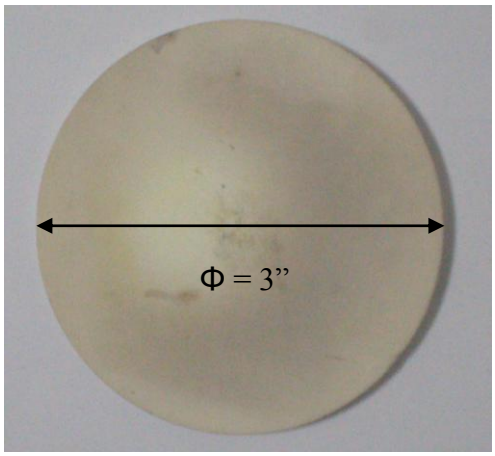

Figure 3.4. Zinc oxide sputtering target.

The deposition rate of the process is approximately 0.7-0.8 nms^{-1}. Sputtering process was performed in an Argon atmosphere with working pressure of 5 x 10^{-3} Torr. The detailed deposition steps are included in appendix A.

3.1.3 Annealing process

Annealing involved a process of heating samples through a certain period of time at a certain temperature in a controlled environment. In this research, the annealing process involves pure nitrogen gas with annealing temperatures of 700^{o}C, 800^{o}C and 900^{o}C. The period of annealing is 2 hours.

A horizontal furnace is used for the annealing process. The Lenton UK Annealing Tube Furnace is shown in figure 3.5.

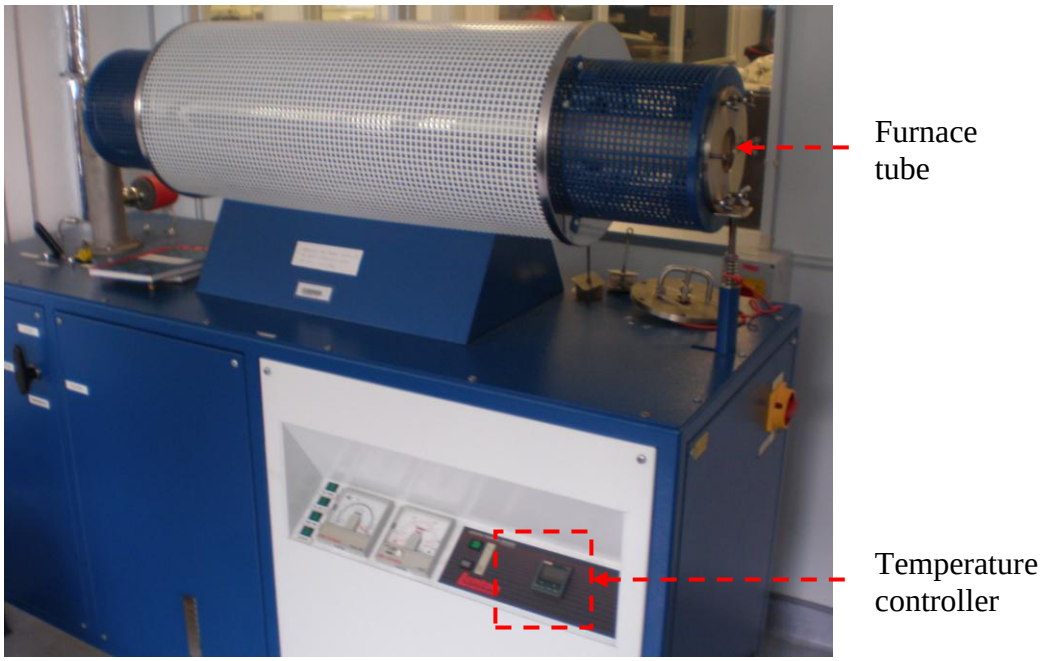

Figure 3.5. The Lenton Furnace.

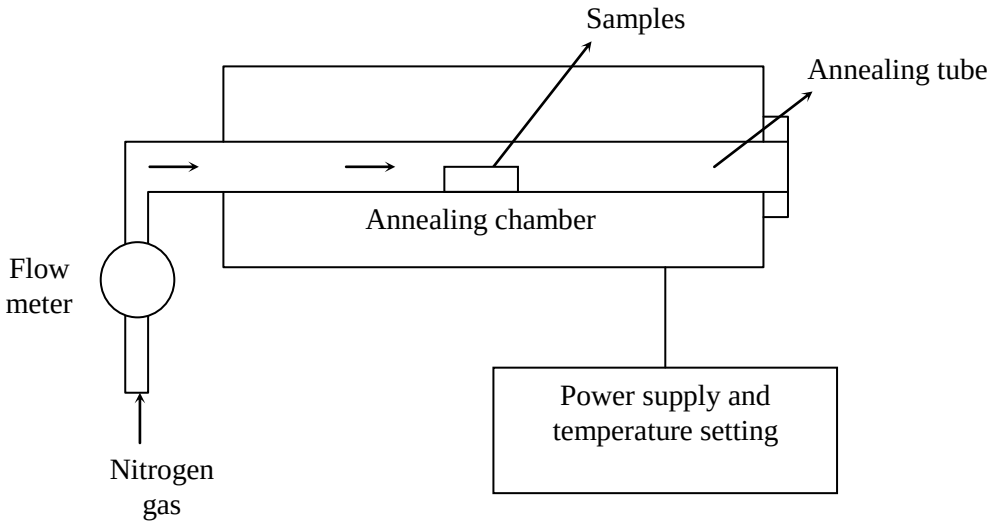

Figure 3.6. Schematic diagram of the Lenton furnace for annealing.

A schematic diagram of the annealing furnace is illustrated in figure 3.6. The arrow showed the nitrogen gas flow through the furnace. Before placing the samples in the center of the annealing tube, the furnace is turn on and annealing temperature is then set. It took approximately half an hour for the furnace to increase temperature from room temperature to 700^{o}C. The nitrogen gas is allowed to flow through the furnace for 15 minutes before the samples were place in the center of the furnace tube to allow the atmosphere in the furnace tube to be displaced by the nitrogen gas. The nitrogen gas flow was set to 4.0 liter/min.

After the furnace has reached the required condition, the samples were placed on a rectangular shape quartz holder and placed in the center of the annealing tube. The samples were annealed at temperatures of 700^{o}C, 800^{o}C and 900^{o}C for a period of 2 hours. During the annealing process, the nitrogen flow is checked from time to time (approximately 20 minutes interval) to ensure the flow rate is maintained at 4.0 liter/min.

After annealing, the samples were carefully taken out of the furnace tube and place on a ceramic to cool down the samples. After the samples were cooled down to